UNIVERSITY OF COPENHAGEN

Bacterial flow cytometry and imaging as potential process monitoring tools for industrial biotechnology

Kadamalakunte Narayana, Sumana; Mallick, Sanjaya; Siegumfeldt, Henrik; van den Berg, Frans

Bacterial Flow Cytometry and Imaging as Potential Process Monitoring Tools for Industrial Biotechnology

Sumana Kadamalakunte Narayana [1],* , **Sanjaya Mallick [2]**, **Henrik Siegumfeldt [1]** and **Frans van den Berg [1]**

[1] Department of Food Science, Faculty of Science, University of Copenhagen, Rolighedsvej 26, DK-1958 Frederiksberg C, Denmark; siegum@food.ku.dk (H.S.); fb@food.ku.dk (F.v.d.B.)

[2] Cytometry Solutions Pvt. Ltd., Balia Main Rd, Garia, Kolkata, West Bengal 700084, India; mallicks@gmail.com

* Correspondence: sumana@food.ku.dk

check for updates

Abstract: Minimizing process variations by early identification of deviations is one approach to make industrial production processes robust. Cell morphology is a direct representation of the physiological state and an important factor for the cell's survival in harsh environments as encountered during industrial processing. The adverse effects of fluctuating process parameters on cells were studied using flow cytometry and imaging. Results showed that altered pH caused a shift in cell size distribution from a heterogeneous mix of elongated and short cells to a homogenous population of short cells. Staining based on membrane integrity revealed a dynamics in the pattern of cluster formation during fermentation. Contradictory findings from forward scatter and imaging highlight the need for use of complementary techniques that provide visual confirmation to interpret changes. An atline flow cytometry or imaging capable of identifying subtle population deviations serves as a powerful monitoring tool for industrial biotechnology.

Keywords: flow cytometry; industrial biotechnology; microscopy; imaging; viability; cell size; forward scatter; *Lactobacillus acidophilus*

1. Introduction

Lactic acid bacteria are one of the most important bacterial species employed in the food industry. They are used as starter cultures in making essential food products like yoghurt, cheese, kefir, wines, etc. [1]. Some lactic acid bacteria like *Lactobacillus acidophilus* are also directly consumed as probiotics due to the health benefits offered by them [2]. The global probiotic market is rapidly growing and was predicted to be valued at USD 77 billion by 2025 [3]. Given the increasing competition among manufacturers, making an industrial probiotic production process efficient and robust is crucial. Reducing the batch-to-batch variations and early identification of unwanted process deviations could assist in this regard [4].

Presently, industries producing probiotics monitor the fermentation process through parameters like pH and amount of base consumed. These are easy-to-get parameters, but often fail to explain the quality or performance variations in the final yield. There are many upstream and downstream possible explanations as to why the probiotic end-product might vary in performance and/or quantity. The formation of zones/gradients in large tanks due to non-ideal mixing is one known issue [5,6]. Lactic acid bacteria are self-acidifiers (they produce lactic acid as a product during growth and thus acidify the medium). In processes involving exponentially growing lactic acid bacteria, zones of low pH can be present locally in the reactor if the rate of external base addition is not sufficient to compensate the

lactic acid formed. As a result, the cells could experience an exposure to changing pH-values as they travel through the different zones in the bioreactor [7].

Cell shape and size (i.e., morphology) are fundamental biological properties. They play an important role in the cell's survival in stressed environments. Primarily, genetic factors determine the morphology of a cell. However, studies have shown that environmental factors such as pH (permanent level changes or shocks), mechanical stress, nutrient starvation during the fermentation process, etc. also have a strong influence on the cell's morphology [8,9]. Many bacteria show morphological changes as a consequence of adapting to stressful conditions [9]. Understanding the cell size distribution and its dynamics under normal process conditions is an important part of process optimization in the biotech industry. E.g., a historical database of cell morphology could be constructed to assist in (long-term) process performance-monitoring and optimization. Unexpected changes occurring due to changing process parameters or gradual cell line changes can be identified using this knowledge.

In this study, two analytical methods–flow cytometry and imaging (both manual and automated)-were used to understand the effect of changing process pH on *Lactobacillus acidophilus* cell morphology. Flow cytometry is a powerful tool, mainly found in research and development laboratories, capable of analyzing multiple physical properties of cells and particles. It records morphological features through light scatter and physiological features through fluorescence signals from the cells. This technique furthermore enables data collection from a large number of isolated events in a very short time span, and thus facilitates the understanding of population characteristics with statistical robustness. This capability is very useful in detecting the occurrence of rare, unwanted events such as cell line deviations. The scatter parameters obtained with a flow cytometer are forward angle scatter (FSC) which varies primarily in accordance with cell size-but factors like refractive index also influence it-and orthogonal/side scatter (SSC) which varies according to the cell's internal complexity and composition. The multiple fluorescence parameters are attributed to the pigments, fluorescent proteins or staining with fluorescent probes, of which the latter can be selected towards a wide array of biochemical properties of the cells [10].

Morphological investigations through imaging techniques like traditional microscopy have been in use in the industry for many years, mostly as a confirmatory quality control method. It often involves analyzing only few samples per batch, collected at certain, specific process steps. Just like flow cytometry, image analysis is usually performed offline i.e., samples collected from the process are transported to a lab facility, and requires skilled technicians for analysis. There are inevitable delays in obtaining the results and manual errors involved. While microscopes have the advantage of revealing intracellular details, the information is only qualitative. It is relatively cumbersome for quantifying the cell counts and cellular characteristics and instruments with higher magnification are needed to obtain high-quality images for such quantitative analysis.

In-situ microscopic probes are now available for noninvasive online morphology monitoring by direct incorporation into the fermenter or process stream [11]. Results are acquired continuously and reported to the control system. However, the high cost and maintenance required make it suitable only for low-volume-high-value biopharmaceutical productions [11]. For high-volume-low-value processes such as probiotics, an atline morphology monitoring (imaging or flow cytometry) is more suitable. An atline method is here defined as one where, the measurements can be performed near the fermenter, by operators. Automated imaging/microscopy has the advantage of recording a higher number of cells per sample (200–5000). It enables determining the cell size distribution, as opposed to traditional microscopy where cell counts are typically limited to around 50–100 cells. Delays due to transport (as for offline modes) and the excessive costs (online modes) are eliminated in the atline analysis. As an intermediate to the two, atline uses simpler equipment compared to the online, and provides quicker results than lab-based offline analysis. An automated imaging system or flow cytometry set-up is a feasible and easy to incorporate solution for industries.

2. Materials and Methods

2.1. Fermentation Process Details

The process under study is a *Lactobacillus acidophilus* fermentation, where the cells are the final product. Commercially available freeze-dried LA-5 cells from Chr. Hansen A/S (Denmark) were used to prepare an overnight culture, and was used as the inoculum. All batch fermentations were performed anaerobically with N_2 purging, at 37 °C in a 2 L bioreactor (working volume 1250 mL).

Autoclaved MRS [12] was the growth media and a starting inoculum of 1% cell inoculum (12.5 mL of overnight culture) was used for all batches. Each fermentation batch was run for a duration of 10 h.

Three different pH regimes were used in this study (Figure 1a). The initial pH of the medium was 6.5 ± 0.2, which gradually drops due to lactic acid production by the growing cells. For a normal batch run, pH control using 1M NH_3 and 1M HCl solutions (Sigma-Aldrich, St. Louis, MO, USA) was started once the pH reached 5.5 to thereafter maintain at this set-point, until the end of fermentation (pH-A). Data from seven batches are investigated in this manuscript, three batches–called normal from here on-were run in pH-A. Two abnormal batches are included which were run at a sub-optimal pH condition of 4.5, from the time pH dropped down to 5.5 until the end of fermentation (pH-B). A third trial trajectory (pH-C) was followed for one test batch, where the batch pH was controlled at 5.5 from time zero, and was gradually lowered (manually) from 5.5 at the start of exponential growth phase (4th hour) to pH 4.5 and maintained there for one hour, after which the pH was bought back to the normal set point of 5.5 at the end of the exponential phase (8th hour). The pH value of 4.5 was chosen with the aim of mimicking the pH stress that could potentially be encountered by the bacteria in large-scale fermenters or in large tanks without proper mixing during holding between different downstream process steps (frequently seen in the industry, caused by e.g., scheduling optimization).

2.2. Biomass Monitoring

Optical density (OD), recorded online during the fermentations using a DenCyte (Hamilton A/S) probe measuring at 880 nm, was used as the measure of total cell counts (un-calibrated for specific cell morphologies, giving relative units/growth profiles, Figure 1b). The probe was calibrated/zeroed against sterile medium, at the start of each batch, before inoculation, in order to negate the background interference.
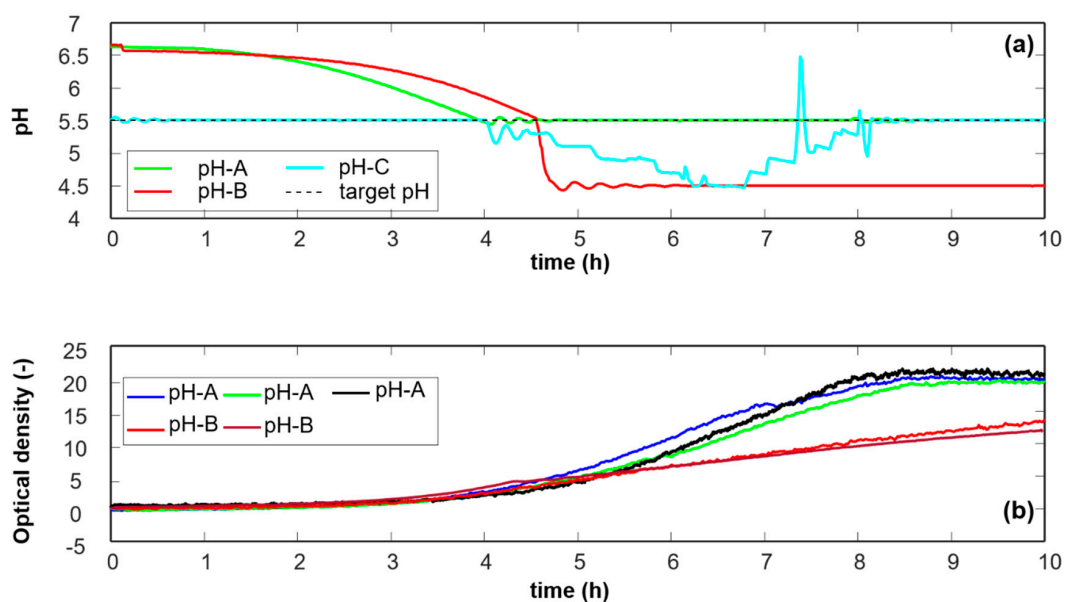

Figure 1. (**a**) Representative pH profiles and (**b**) OD profiles for three pH-A batches and two pH-B batches run in 2 L bioreactor.

2.3. Flow Cytometry

2.3.1. Flow Cytometer Settings

All flow cytometry analysis were performed using a BD FACSJazz^{TM} cell sorter, which uses a 488nm argon ion laser as the light source. Rainbow Calibration Particles (8 peaks, 3.0 to 3.4 μm) from BD Biosciences were used for laser alignment each day before analysis. The forward scatter (FSC) signal was collected in the direction of the laser and side scatter (SSC) at a 90° angle to the laser. FSC versus SSC plots were used as reference to ensure recoding of the right bacterial population. Fluorescence was collected in two channels–green fluorescence from SYTO9 stained cells (called FL_1 from here on) with a band-pass filter of 530 ± 20 nm and red fluorescence from PI stained cells (FL_2) with a band-pass filter of 692 ± 20 nm. Sheath fluid from BD FACSFlow™ was used at a flow rate of 0.5 L·h^{-1} and the event count for each recording was set to 100,000. Milli-Q water was run in-between samples until the event count was below 100 per second to ensure no carry over from one sample to the next.

2.3.2. Sample Preparation, Cell Staining, and Data Analysis

5 mL of fermentation broth was withdrawn aseptically from the fermenter every hour, 1 mL of which was centrifuged using a bench-top micro centrifuge (LLG labware, Meckenheim, Germany) to separate the spent media from the cells. Centrifuged supernatant was discarded and the cell pellets were stored at 4 °C until analysis. 1 mL of 0.85% NaCl solution was used to re-suspend the cells prior to flow cytometric analysis.

A LIVE/DEAD^{TM} bacterial viability kit from ThermoFisher Scientific (Waltham, MA, United States), consisting of Propidium iodide (PI) and SYTO9, which stain the cells selectively based on membrane integrity, was used. All sample preparation and staining protocols were followed as per the kits instructions [13]. Viability analysis by cell staining was performed for most samples in pH-A and pH-B, while in pH-C staining was only done for selected samples.

All '.fcs' data files from the flow cytometry instrument were read and analyzed using MATLAB scripts. In-house MATLAB code and the image processing toolbox were used to make density plots of FL_1 against FL_2 signals and to manually pick the number of clusters, and initial cluster center. Once this initiation was done, all events belonging to one cluster were included by manually adjusting the (hexagonal) boundary of the cluster marked, after which the center was recalculated. Data processing with the above method was used for all recordings to extract the percentage of the total counts for each cluster.

2.4. Imaging Techniques for Morphology Analysis

2.4.1. Microscopic Analysis

To appreciate the correlation between cell size and flow cytometry FSC, microscopic analysis was performed using a bright field oil-immersion light microscope with 60× magnification. 1 mL of the hourly sample was centrifuged to remove the supernatant, and cells were re-suspended in 0.85% NaCl buffer for dilution. Approximately 10 μL of sample was pipetted onto a microscopic glass slide, covered with gel pads (made from 5% agarose) and digital images were recorded for evaluation.

2.4.2. Automated Cell Imaging Analysis

The oCelloScope^{TM} (BioSense Solutions ApS, Farum, Denmark) was used for the morphology analysis in *atline* mode. Samples were presented to the instrument on a 96-well plate, where 100 μL of diluted sample (in 0.85% NaCl buffer) was pipetted onto each well. Dilution level was determined based on the cell concentration in the batch. For the first hours, undiluted samples worked well; while in the later hours (higher biomass), the samples were diluted to make sure that individual cells could be accurately quantified by the morphological descriptors (in the digital images). For image acquisition, default settings on the oCelloScope^{TM} with auto-illumination plus 2 ms illumination time

were used. Number of images used was 10 and recording was done at a distance of 10 μm above the plate bottom. Built-in segmentation analysis from the instrument software (BioSense Solutions ApS, Farum, Denmark) was used to extract few features to describe the cell morphology-circularity, and cell skeleton length [14].

3. Results

3.1. pH Effect on Biomass Formation and Growth

The primary focus in this study was to investigate the effects of pH alterations that can potentially occur during an industrial-scale fermentation on bacterial cell size/morphology, its distribution and cell viability. A significantly lower final cell density–based on OD measurements–was observed when cells were grown in experimental conditions pH-B, as opposed to the normal pH-A, as shown in Figure 1b. The difference in biomass is a reflection of the stress encountered during the process.

3.2. Cell Size Dynamics

Understanding the cell size distribution and its dynamics under normal process conditions is an important part of process optimization in the biotech industry. For example, a historical database of cell morphology could be constructed to assist in (long-term) process performance-monitoring and optimization. Unexpected changes occurring due to the changing process parameters or gradual cell line changes can be identified using this knowledge. In our study, change in the light scatter collected at the FSC channel was used to investigate the effect of changed pH on cell size distribution. Figure 2 shows the normalized FSC histograms for the pH-A and pH-B batches. For pH-A, a clear, systematic trend in the development of two (or possible more) subpopulations from one common starting population is observed, i.e., a broad range of cell sizes towards the end of fermentation is seen. The two distinct but overlapping subpopulations, can be interpreted as small and elongated cells existing in an actively growing and dividing cell population. In contrast, pH-B batches showed a distinct, narrower, and more homogenous cell population towards the end of the fermentation.
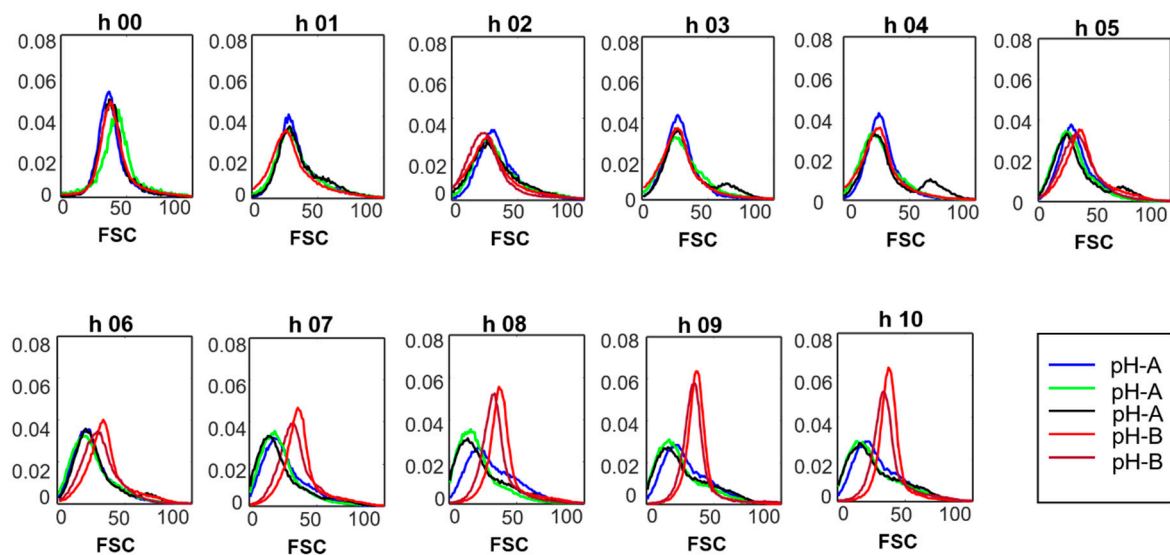

Figure 2. Forward scatter signal (normalized) for samples analyzed every hour during the fermentation.

For a better understanding of the differences in FSC signals and correlate them to actual cell size, microscopic imaging of cells was performed. Figure 3 shows the recordings for samples at the last hour for pH-A (Figure 3a) and pH-B (Figure 3b); the images are representative for the general trends observed. The statistical moments for cell area extracted from microscopic images are reported in

Table 1. The images in Figure 3 reveal that the cells in pH-B are considerably smaller than those in pH-A, and that the population in pH-B is rather homogenous in comparison to pH-A.
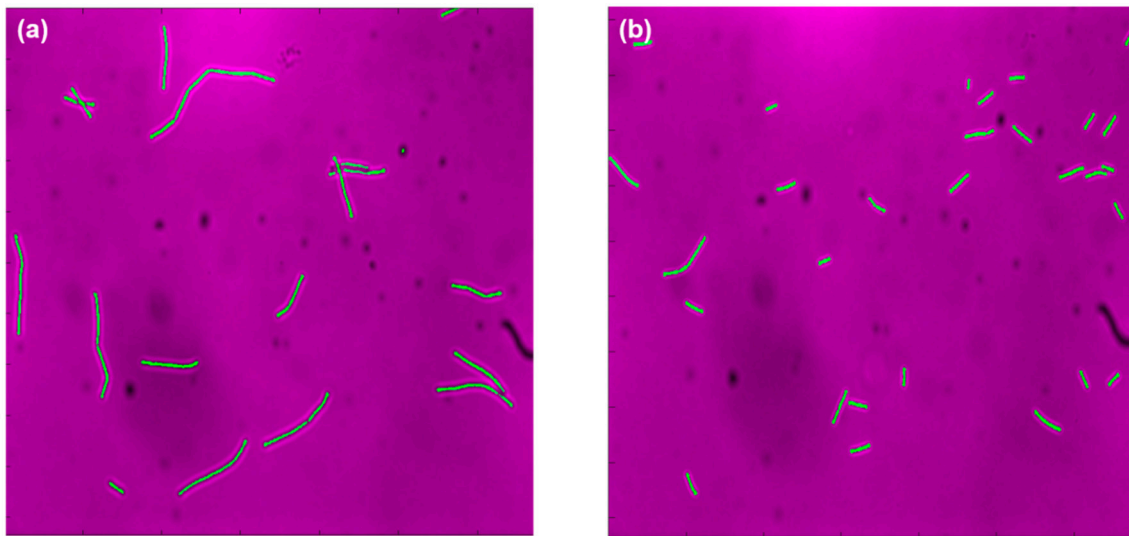

Figure 3. Microscopic images (false color) for 10th hour sample taken from (**a**) pH-A and (**b**) pH-B.

Table 1. Statistical moments for cell area (in pixels) extracted from microscopic and automated images of final-hour fermentation samples from pH-A and pH-B.

	Microscope		Automated Imaging	
	pH-A	**pH-B**	**pH-A**	**pH-B**
Object counts	129	160	390	845
Mean	518	328	41	16
Median	440	326	35	12
Std Dev [a]	439	187	31	14
IQR [b]	758	458	53	21

[a]—Standard deviation, [b]—Inter-quartile range.

The results from automated imaging were similar to that from microscopy. Two representative images obtained from the automated imaging system are shown in Figure 4. These images also showed a heterogeneous population in pH-A (Figure 4a) in contrast to a homogenous population with smaller cells for pH-B (Figure 4b). The areas extracted from all images taken during this investigation are reported in Table 1 and give the confirming interpretation that pH-B results in smaller cells. Figure 5 shows normalized histograms for two morphological features–circularity and cell length-extracted from automated images for samples at the 5th and 10th hour of fermentation. It can be seen that at the 5th hour of fermentation (Figure 5a,c), the cell populations in pH-A and pH-B are almost similarly distributed. Towards the end of fermentation (Figure 5b,d), the two populations are clearly different-pH-B has many shorter, more circular cells while pH-A has longer, elongated cells with a wider range of cell lengths. Although both the features distinguish the pH-A and pH-B cells, distinction between the populations is clearest via circularity (Figure 5b) in comparison to the cell length (Figure 5d).
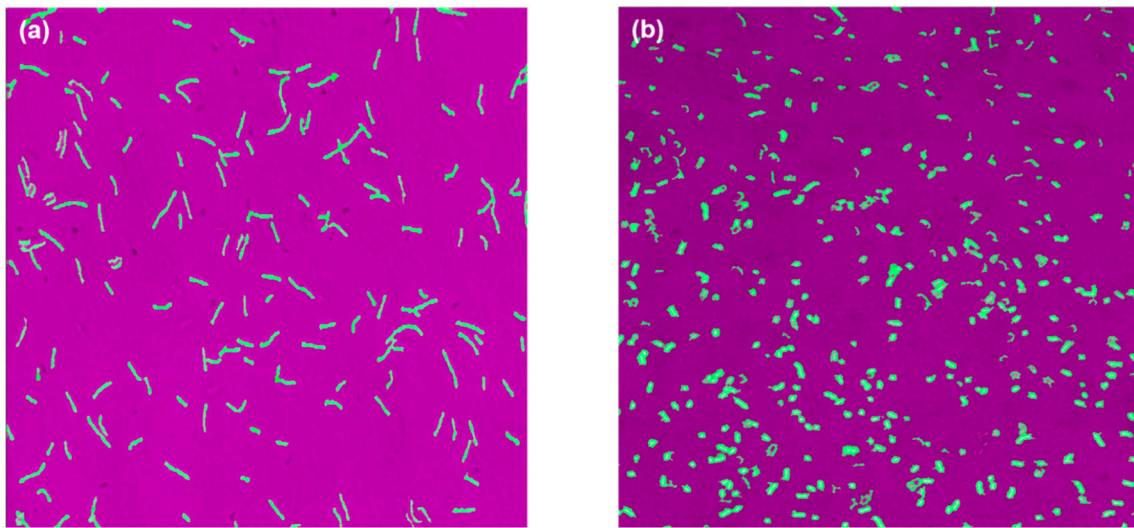
Figure 4. Automated (oCelloScope^TM) images for 10th hour samples taken from (**a**) pH-A and (**b**) pH-B.
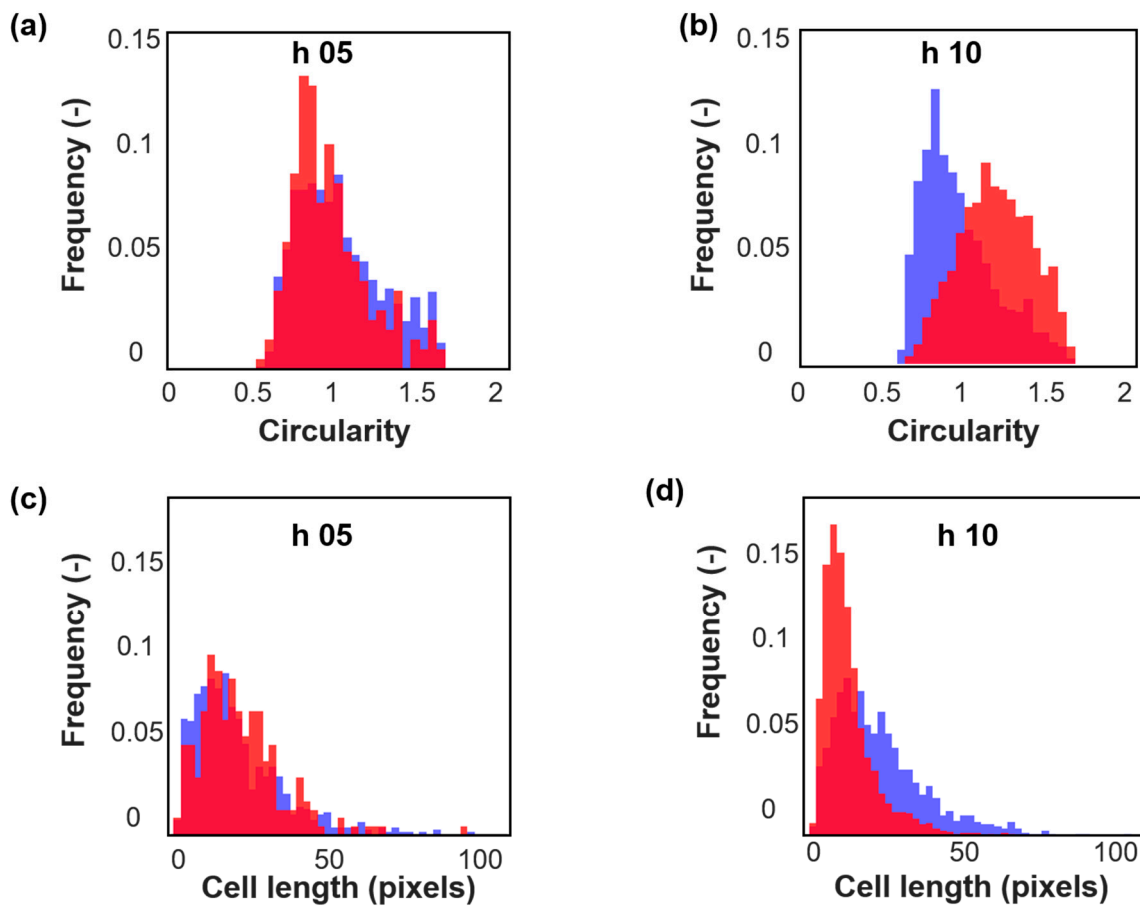

Figure 5. Normalized histograms for (**a**) circularity, 5th hour samples; (**b**) circularity, 10th hour samples; (**c**) cell length 5th hour samples; and (**d**) cell length 10th hour samples from one representative pH-A (blue) and pH-B (red) batch.

The most striking observation when comparing results from flow cytometry and imaging was that the actual size of cells in pH-B are much smaller and shorter (Figures 3b and 4b) than the ones in pH-A (Figures 3a and 4a) while the FSC signals give the opposite impression i.e., that pH-B results in larger cells (Figure 2). To understand this anomaly in the scatter results, the trigger pulse width distributions were plotted in Figure 6a. The contrast between trigger pulse width (Figure 6a) and FSC

(Figure 6b) can be seen from the statistical moment-values in Table 2. From these trigger width values, it is clear that pH-B cells are indeed smaller compared to pH-A cells.
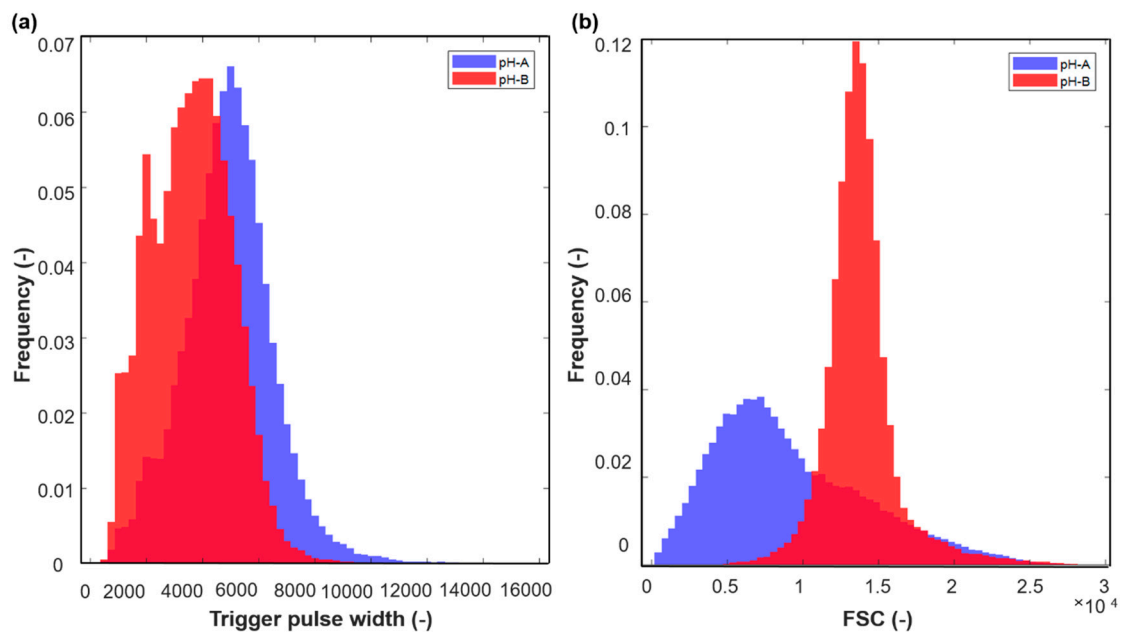

Figure 6. Normalized histograms of (**a**) flow cytometry trigger pulse width (**b**) forward scatter (FSC) signal for 10th hour samples taken from a representative pH-A and pH-B batch.

Table 2. Statistical moments for flow cytometry (100,000 events) forward angle scatter/FSC (arbitrary units) and trigger pulse width (arbitrary units) of final-hour fermentation samples from pH-A and pH-B.

	FSC		Trigger-Pulse Width	
	pH-A	**pH-B**	**pH-A**	**pH-B**
Mean	9237	13809	4925	3608
Median	8180	13620	4934	3620
Std Dev [a]	5068	2384	1641	1442
IQR [b]	12418	14677	5860	4611

[a]—Standard deviation, [b]—Inter-quartile range.

3.3. Viability Analysis

The multi-parametric nature of flow cytometry allows for investigation of cell viability next to size, through fluorescent staining. In this study, the common interpretation was used that cells with an intact, tight cell membrane are alive, and cells with porous/damaged cell membrane are dead. The recorded events were divided into three distinct clusters based on the difference in PI/SYTO9 staining intensity (no compensation was used). The clusters were quantified using in-house scripts, two representative examples are shown in Figure 7. Cluster C_1 is composed of cells with higher green than red fluorescence, stained mainly by SYTO9. The cells that make up cluster C_2 had approximately equal amounts of red and green fluorescence and are identified as damaged cells (or cells with a more fluid cell membrane), which allow both PI and SYTO9 to stain them. Finally, the cells in cluster C_3 have higher red than green fluorescence and are identified as dead or membrane compromised cells. From here onwards, C_1 is therefore considered as the live cluster, C_2 as the intermediate cluster and C_3 as the dead cluster. Microsphere beads with pre-defined green and red fluorescence can be seen as the fixed population in cluster C_4 (in Figure 7a). Percentage of live, damaged and dead cells for three pH-A batches, one pH-B batch, and trail run pH-C are reported in Table 3.
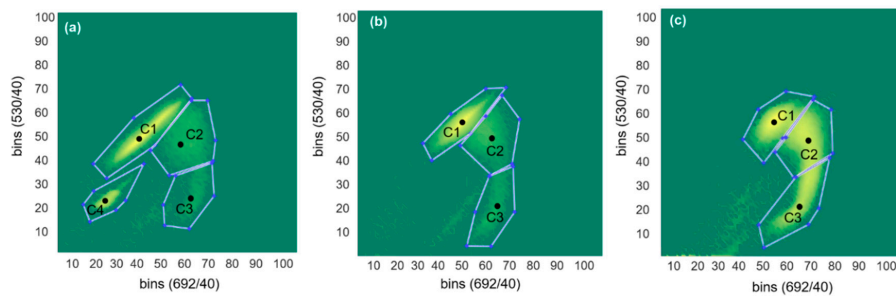
Figure 7. Plot of FL_1 against FL_2 fluorescence intensities showing four clusters (C1-live, C2-intermediate, C3-dead and C4-beads) identified using MATLAB scripts for (**a**) 10th hour sample from pH-A, (**b**) 10th hour sample from pH-B and (**c**) 7th hour sample from pH-C.

The staining revealed a dynamics in the cluster formation and the group-shapes changed over batch time, an example of which is shown in Figure 8. We did not observe noticeable differences in live cell percentages due to stressing the cells in an acidic pH of 4.5 (pH-B). Special test batch pH-C on the other hand, caused the live cell percentage to drop drastically to 29% at the 7th hour (Figure 7b) and a slow (but gradual) improvement was observed when the pH was shifted back to 5.5 at the 8th hour (Table 3). Plating results also showed fewer cells at the end of fermentation in pH-B as compared to pH-A (Table 4).
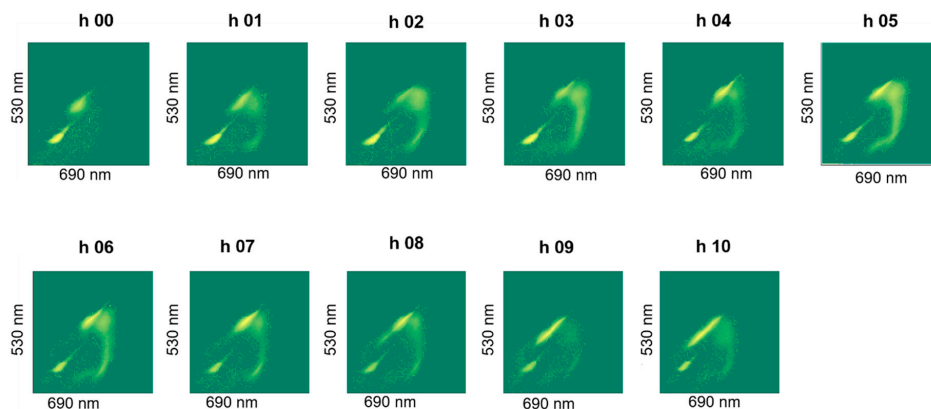

Figure 8. Plot of FL_1 against FL_2 fluorescence intensities of hourly samples showing dynamics of clusters observed during fermentation, shown for one representative pH-A batch (Plots for other batches shown in Appendix A).

Table 3. Percentage event counts from clusters C_1 (live)/C_2 (intermediate)/C_3 (dead).

Time (h)	pH-A			pH-B	pH-C
	(1)	(2)	(3)	(1)	(1)
0	99/00/01	86/14/00	100/00/00	96/04/00	- [a]
1	76/17/06	27/35/38	76/20/05	62/20/08	80/12/08
2	28/57/14	20/62/18	43/45/11	47/41/12	-
3	35/55/09	26/64/09	60/36/04	26/48/26	-
4	91/06/04	71/23/06	82/12/06	36/56/08	88/09/03
5	69/23/08	75/20/05	64/07/29	64/34/02	77/14/09
6	71/18/10	72/24/03	61/23/16	74/22/04	77/20/03
7	88/07/05	61/31/08	73/18/09	69/26/05	29/44/27
8	90/07/03	73/19/08	64/22/13	78/14/07	35/45/20
9	98/01/01	95/05/01	88/09/03	94/04/01	55/30/14
10	94/05/01	92/07/01	80/14/06	93/05/02	78/13/09

[a]—Flow cytometry staining analysis not performed for these hours and second pH-B experiment.

Table 4. Average colony forming unit (CFU) counts for zero and final-hour fermentation samples from pH-A and pH-B.

Time (h)	pH-A	pH-B
h 00	2.23×10^8	1.04×10^9
h 10	2.41×10^{12}	4.00×10^{10}

4. Discussion

Industrial bioprocessing includes several downstream steps following the fermentation step. During processing, due to practical reasons such as low capacity of the equipment or (unpredictable) time lags between the operating steps could result in hold up of the cells in large tanks, (typically) without proper mixing or pH control. High density lactic acid cultures can rapidly lower the pH and cause an adverse effect on the live cell percentage (as seen in pH-C). This would cause a loss of product and potentially noticeable economic consequences. Use of better monitoring tools on the work floor can thus, not only detect deviating cell size distributions, but also identify changes in viability in the case of flow cytometry and help improve process productivity.

Lactic acid bacteria are known to be resistant to pH stresses [15]. The behavior observed in pH-B, where the cells adapt to the new environment and maintain good viability until the end of fermentation, is therefore maybe not very surprising. Although *L. acidophilus* are known to survive under lower pH conditions, a drop in pH from the set point would induce an unwanted stress to the cells. Studies have revealed that the cells strive to maintain a neutral pH inside, by pumping excessive protons (introduced by the low pH of the medium) out of the cell, thereby diverting the energy available towards maintenance rather than forming new cells [16]. The lower biomass obtained in pH-B (Figure 1b, Table 4) was interpreted as a manifestation of the cell's survival in altered pH conditions.

Bacterial stress response includes a wide variety of metabolic and physiological changes, including formation of inactive spores, shift into dormant states like viable-but-non-culturable (VBNC) states [8,17] and pleomorphism i.e., change of cell shape and size. The shift in cell size distribution as observed in the case of pH-B is a known response/survival strategy. Phenotypic heterogeneity of a population is a well-known strategy that allows for survival and functionality of the microorganism under stressful environmental conditions [18,19]. The importance of cell shape and size for the survival of bacteria in case of threats like nutrient depletion or pH stresses and the resulting morphological changes has been discussed in literature [9,20]. Several examples of cells changing size in response to the encountered stress are available. This includes studies such as *Bifidobacterium* changing their shape due to stress [21], and *L. bulgaricus* increasing chain length and shifting from rod shaped to filamentous form by inhibiting cell division upon encounter with alkaline pH [22] etc.

The unexpected, contrasting results obtained from FSC and imaging techniques while analyzing the changes in cell size distribution, highlight the significance of using complementary analytical techniques in process understanding. According to convention, forward scattered light in the small angle region ($\theta \leq 2°$, where $\theta = 0°$ corresponds to the direction of incident light) is primarily dependent on the cell's size and refractive index [23]. Accordingly, the changed FSC observed in pH-B could be naively interpreted as increase in cell size. However, other parameters such as cell shape, refractive index and density are important factors contributing to the forward scatter generated by the cell [24]. Therefore, a linear relation cannot always be expected between FSC signals and cell size [25,26]. The pulse width is a parameter recorded by the flow cytometer that reflects the electric pulse created at the detector when a cell passes through the laser. Rod-shaped cells such as *L. acidophilus* have a tendency to be aligned (by the hydrodynamic focusing of the cytometer) along their long-axis when traveling through the laser [27,28]. Therefore, the pulse width parameter is an indication of travel time required and this value increases with cell length (for the cells used here).

Many studies suggest that light scattered from biological particles (cells) depends on other cellular properties such as refractive index, density, and orientation in addition to the size [24,29]. Kerker and

co-authors [24] describe the dependence of light scatter by cells on refractive index in detail. Another recent study by Liu and co-authors [30] suggests that the average refractive index of a cell suspension depends on the volume fraction of cells. Using these investigations as guidelines, it was inferred here that for pH-B, the reduced size of the cells reduces the volume fraction and in turn, results in an increased refractive index of the cell suspension [30]. Further, the increased refractive index (from the decreased cell size) is reflected as increased FSC signal from the pH-B cells. Combining this with the results from imaging and trigger pulse width, we confirm that pH-B caused shrinking of the cells. However, it is important to note that the effects of the shifted cell size distribution on cell resistance to stress caused during further (downstream) processing steps have to be evaluated separately.

While microscopic images show the true state of cells, automated imaging systems are comparatively inexpensive, and practically provide the same type of information (cell shape and size). In addition to acting as a confirmatory technique to FSC, the results from automated imaging depict here that analyzing multiple cellular features such as circularity, elongation etc., that are not readily detected in traditional microscopy provides a means for easier identification of small changes in the cell populations.

5. Conclusions

The focus of this study was to understand the impact of altered pH conditions, which could potentially occur in an industrial probiotic production process, on cell morphology and product quality. The two analytical techniques used in this study to assess morphology-flow cytometry and imaging (manual and automated)-complemented each other and helped understand the manifestation of pH effect on the cells. Contrary to the conventional interpretation that cells with bigger size give higher FSC, we observed that smaller, denser cells resulting from a shift in pH to 4.5, showed higher FSC numbers. The results emphasize the need to understand the principle that FSC does not depend on cell size only, but other factors as well like refractive index, angle of scatter collection, etc. Therefore, using only FSC to analyze cell size could be misleading. The distinct shift in cell size distribution towards a homogenous population seen in both the FSC signals from flow cytometry and images reflect the impact of changed pH. Manifestation of the changed population heterogeneity on the cell's survival in downstream process steps could be significant.

In addition, OD and CFU analysis confirmed that the reduced values of OD and CFU counts in pH-B indicate that acidic conditions occurring within fermenters could be harmful to the cells and result in reduced final cell density at the end of fermentation. While neither OD nor flow cytometry could be used individually to describe the effect of pH on the cells, combining OD and percentage alive from flow cytometry gives a better/reliable count of the amount of live cells in a fermentation harvest. The viability counts also showed that a constant exposure to a lower than optimal pH (here represented by the somewhat extreme value 4.5, simulating the industrial scale pH gradients) is far less lethal in comparison to a continuously changing/dropping pH (that could result from holding of the product between process steps).

The clear shift in cell size distribution from heterogeneous to homogenous under the changed pH is a stress response. The cells produced from the processes operated at suboptimal pH could have lower resistance to future stress or may have longer lag periods. Investigations such as the one performed here are already included in process design and up-scaling experiments in the biotech industry. However, for daily performance monitoring they are too costly, or more generally, too involved. Identifying such shifts in cell size distributions occurring during fermentation, over many batches, could prove to be crucial in reducing loss of viable cells in the freeze-drying step. Flow cytometry gives a deeper insight into the process by describing not only the morphology of the culture at any time point, but also quantifying the viable cell counts. The results from our study indicate that an atline implementation of morphology analysis with flow cytometry or automated imaging could prove to be valuable in detecting such process deviations that could otherwise go unnoticed.

Image analysis is possibly the more attractive and competitive process analytical tool for industrial biotechnology mainly due to its atline applicability, real-time results and simple nature as opposed to the currently available traditional, post-quality-control methods like plating. In our results, both microscopic and automated images showed similar findings. This indicates that newer, automated imaging systems, which are less expensive and easier to handle, compared to microscopes can be implemented for routine, quick checking of samples on the work floor. At the cost of some operator time, they are easy-to-use and can be performed by nearly everybody, without the need of highly trained personnel as in the case of microscopy. Imaging techniques provide visual confirmation of the cellular characteristics. Although imaging does not provide the same process insight as flow cytometry, the morphological distribution information might be sufficient, especially after a (laboratory-based) comparison within a bacterial strain is available. Atline imaging is a powerful, affordable, user-friendly process monitoring tool for industrial biotechnology.
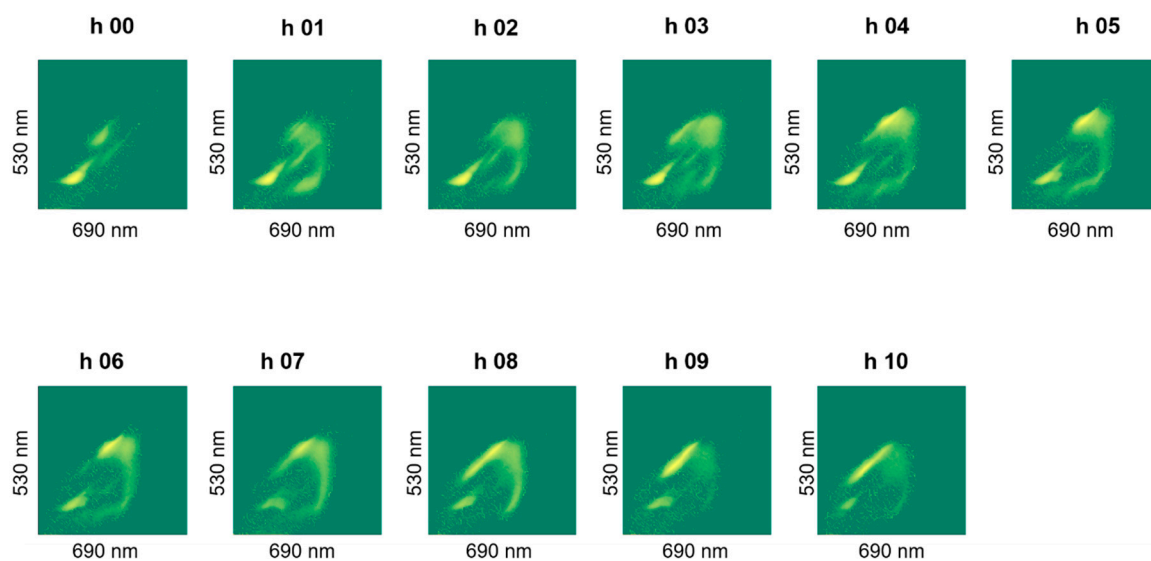
Appendix A

Figure A1. Plot of FL_1 against FL_2 fluorescence intensities of hourly samples showing dynamics of clusters observed during fermentation for pH-A (2) batch.
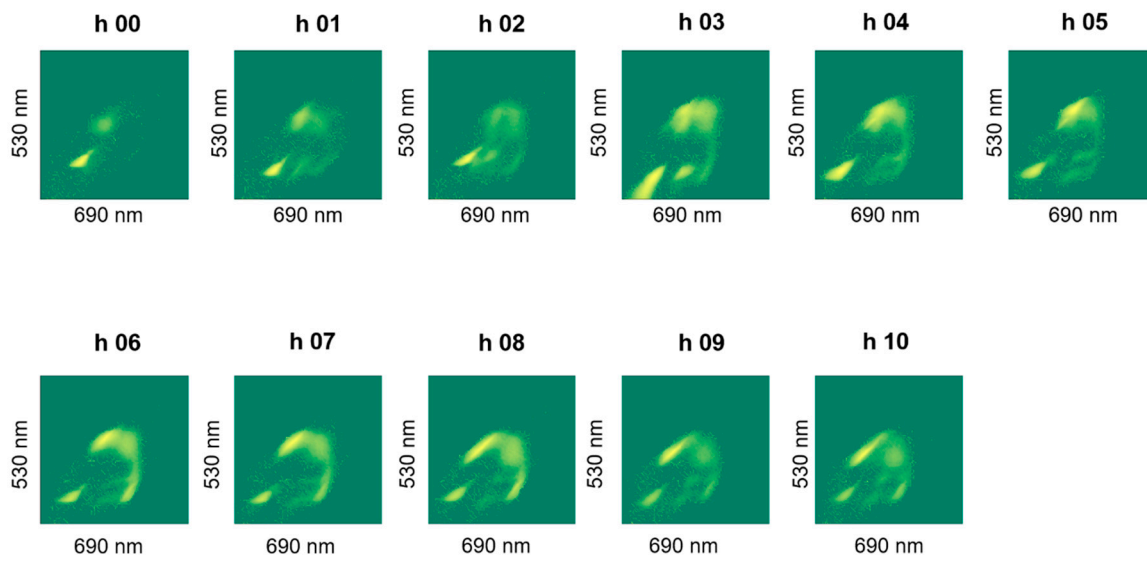
Figure A2. Plot of FL_1 against FL_2 fluorescence intensities of hourly samples showing dynamics of clusters observed during fermentation for pH-A (3) batch.
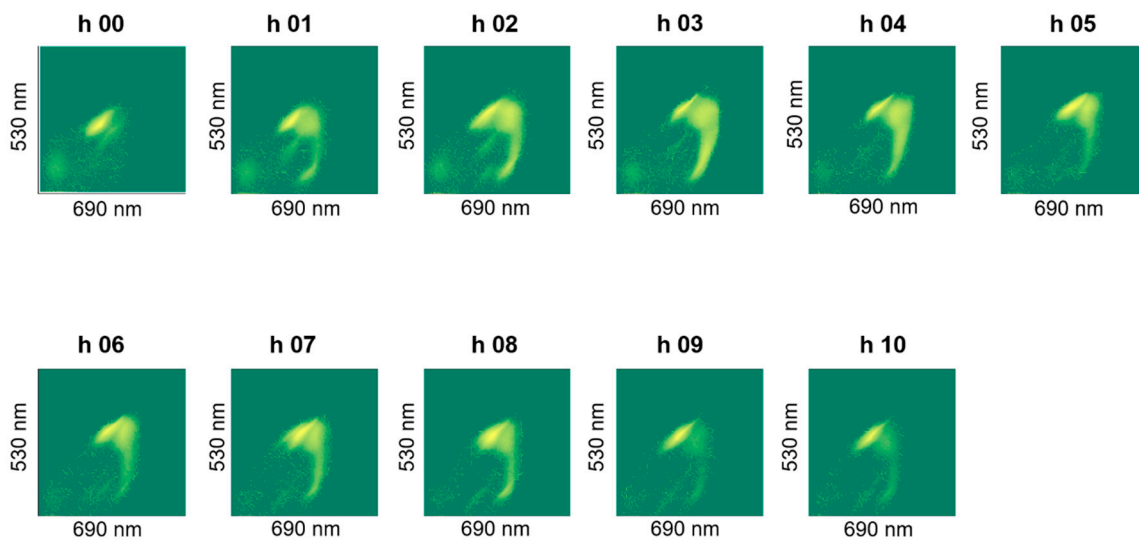

Figure A3. Plot of FL_1 against FL_2 fluorescence intensities of hourly samples showing dynamics of clusters observed during fermentation for pH-B (1) batch.

Figure A4. Plot of FL_1 against FL_2 fluorescence intensities of hourly samples showing dynamics of clusters observed during fermentation for pH-C (1) batch.
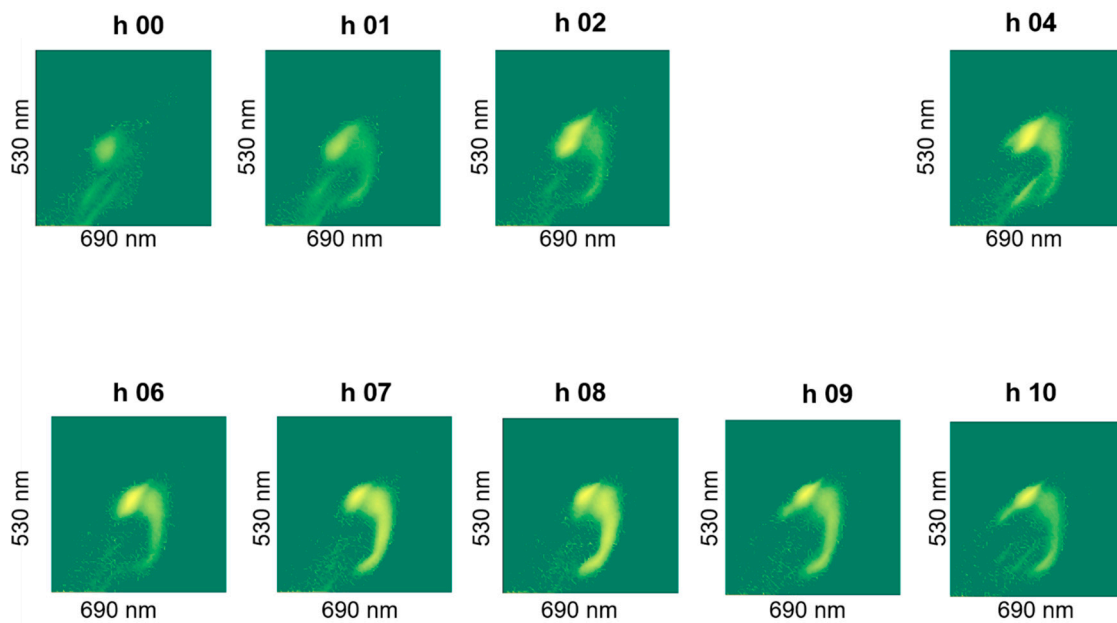
References

1. Leroy, F.; De Vuyst, L. Lactic acid bacteria as functional starter cultures for the food fermentation industry. *Trends Food Sci. Technol.* **2004**, *15*, 67–78. [CrossRef]
2. Bigret, M.; Mäyrä-Mäkinen, A. Industrial Use and Production of Lactic Acid Bacteria. *Lact. Acid Bact.* **2004**. [CrossRef]
3. Research, G. View Probiotics Market Worth $77.09 Billion By 2025. Available online: https://www.grandviewresearch.com/press-release/global-probiotics-market (accessed on 14 September 2019).
4. Narayana, S.; Christensen, L.; Skov, T.; van den Berg, F. Mid-Infrared Spectroscopy and Multivariate Analysis to Characterize Lactobacillus acidophilus Fermentation Processes. *Appl. Spectrosc.* **2019**, *73*, 1087–1098. [CrossRef]
5. Spann, R.; Glibstrup, J.; Pellicer-Alborch, K.; Junne, S.; Neubauer, P.; Roca, C.; Kold, D.; Lantz, A.E.; Sin, G.; Gernaey, K.V.; et al. CFD predicted pH gradients in lactic acid bacteria cultivations. *Biotechnol. Bioeng.* **2018**, *116*. [CrossRef]
6. Carlquist, M.; Fernandes, R.; Helmark, S.; Heins, A.-L.; Lundin, L.; Sørensen, S.J.; Gernaey, K.V.; Lantz, A. Physiological heterogeneities in microbial populations and implications for physical stress tolerance. *Microb. Cell Fact.* **2012**, *11*, 94. [CrossRef]
7. Enfors, S.O.; Jahic, M.; Rozkov, A.; Xu, B.; Hecker, M.; Jürgen, B.; Krüger, E.; Schweder, T.; Hamer, G.; O'Beirne, D.; et al. Physiological responses to mixing in large scale bioreactors. *J. Biotechnol.* **2001**, *85*, 175–185. [CrossRef]
8. van Teeseling, M.C.F.; de Pedro, M.A.; Cava, F. Determinants of bacterial morphology: From fundamentals to possibilities for antimicrobial targeting. *Front. Microbiol.* **2017**, *8*, 1–18. [CrossRef]
9. Yang, D.C.; Blair, K.M.; Salama, N.R. Staying in Shape: The Impact of Cell Shape on Bacterial Survival in Diverse Environments. *Microbiol. Mol. Biol. Rev.* **2000**, *80*, 187–203. [CrossRef]
10. Adan, A.; Alizada, G.; Kiraz, Y.; Baran, Y.; Nalbant, A. Flow cytometry: Basic principles and applications. *Crit. Rev. Biotechnol.* **2017**, *37*, 163–176. [CrossRef]
11. Joeris, K.; Frerichs, J.G.; Konstantinov, K.; Scheper, T. In-situ microscopy: Online process monitoring of mammalian cell cultures. *Cytotechnology* **2002**, *38*, 129–134. [CrossRef]
12. De Man, J.C.; Rogosa, M.; Sharpe, M.E. A Medium For The Cultivation Of Lactobacilli. *J. Appl. Bacteriol.* **1960**, *23*, 130–135. [CrossRef]
13. *Protocols LIVE/DEAD® Bac Light^{TM} Bacterial Viability and Counting Kit (L34856) (Flow Cytometry Kit)*; ThermoFisher: Waltham, MA, USA, 2004.

14. BioSense Solutions. *oCelloScope Technology*; BioSense Solutions: Farum, Denmark, 2017.

15. Hussain, M.A.; Hosseini Nezhad, M.; Sheng, Y.; Amoafo, O. Proteomics and the stressful life of lactobacilli. *FEMS Microbiol. Lett.* **2013**, *349*, 1–8. [CrossRef] [PubMed]

16. Šušković, J.; Kos, B.; Beganović, J.; Pavunc, A.L.; Habjanič, K.; Matoć, S. Surviving the Acid Test: Responses of Gram-Positive Bacteria to Low pH. *Food Technol. Biotechnol.* **2010**, *48*, 296–307.

17. Davis, K.M.; Isberg, R.R. Defining heterogeneity within bacterial populations via single cell approaches. *BioEssays* **2016**, *38*, 782–790. [CrossRef] [PubMed]

18. De Jong, I.G.; Haccou, P.; Kuipers, O.P. Bet hedging or not? A guide to proper classification of microbial survival strategies. *BioEssays* **2011**, *33*, 215–223. [CrossRef]

19. Van Boxtel, C.; Van Heerden, J.H.; Nordholt, N.; Schmidt, P.; Bruggeman, F.J. Taking chances and making mistakes: Non-genetic phenotypic heterogeneity and its consequences for surviving in dynamic environments. *J. R. Soc. Interface* **2017**, *14*. [CrossRef]

20. Cesar, S.; Huang, K.C. Thinking big: The tunability of bacterial cell size. *FEMS Microbiol. Rev.* **2017**, *41*, 672–678. [CrossRef]

21. Macfarlane, G.; Cummings, J. Probiotics and prebiotics: Can regulating the activities of intestinal bacteria benefit health? *BMJ* **1999**, *318*, 999–1003. [CrossRef]

22. Rhee, S.K.; Pack, M.Y. Effect of environmental pH on fermentation balance of Lactobacillus bulgaricus. *J. Bacteriol.* **1980**, *144*, 217–221. [CrossRef]

23. Mullaney, P.F.; Van Dilla, M.A.; Coulter, J.R.; Dean, P.N. Cell sizing: A light scattering photometer for rapid volume determination. *Rev. Sci. Instrum.* **1969**, *40*, 1029–1032. [CrossRef]

24. Kerker, M.; Chew, H.; McNulty, P.J.; Kratohvil, J.P.; Cooke, D.D.; Sculley, M.; Lee, M.P. Light scattering and fluorescence by small particles having internal structure. *J. Histochem. Cytochem.* **1979**, *27*, 250–263. [CrossRef] [PubMed]

25. Lopez-Amoros, R.; Comas, J.; Carulla, C.; Vives-Rego, J. Variations in flow cytometric forward scatter signals and cell size in batch cultures of Escherichia coli. *FEMS Microbiol. Lett.* **1994**, *117*, 225–229. [CrossRef]

26. Müller, S.; Nebe-Von-Caron, G. Functional single-cell analyses: Flow cytometry and cell sorting of microbial populations and communities. *FEMS Microbiol. Rev.* **2010**, *34*, 554–587. [CrossRef] [PubMed]

27. Pinder, A.C.; Purdy, P.W.; Poulter, S.A.G.; Clark, D.C. Validation of flow cytometry for rapid enumeration of bacterial concentrations in pure cultures. *J. Appl. Bacteriol.* **1990**, *69*, 92–100. [CrossRef]

28. Kachel, V.; Fellner-Feldegg, H.; Menke, E. Hydrodynamic properties of flow cytometry instruments. In *Flow Cytometry and Sorting*; Melamed, M.R., Lindmo, T., Mendelsohn, M.L., Eds.; John Wiley & Sons Ltd.: New York, NY, USA, 1990; pp. 27–44.

29. Watson, D.; Hagen, N.; Diver, J.; Marchand, P.; Chachisvilis, M. Elastic light scattering from single cells: Orientational dynamics in optical trap. *Biophys. J.* **2004**, *87*, 1298–1306. [CrossRef]

30. Liu, P.Y.; Chin, L.K.; Ser, W.; Chen, H.F.; Hsieh, C.M.; Lee, C.H.; Sung, K.B.; Ayi, T.C.; Yap, P.H.; Liedberg, B.; et al. Cell refractive index for cell biology and disease diagnosis: Past, present and future. *Lab Chip* **2016**, *16*, 634–644. [CrossRef]